

Reduction in the resident intestinal myelomonocytic cell population occurs during *Apc*^{Min/+} mouse intestinal tumorigenesis

OLUSOLA O. FALUYI¹⁻³, MARK A. HULL¹, ALEXANDER F. MARKHAM¹,
 CONSTANZE BONIFER⁴ and P. LOUISE COLETTA¹

¹Section of Molecular Gastroenterology, Leeds Institute of Medical Research, University of Leeds, St. James's University Hospital, Leeds, Yorkshire LS9 7TF; ²Experimental Cancer Medicine Centre, Clatterbridge Cancer Centre NHS Foundation Trust, Bebington, Wirral, Merseyside CH63 4JY;

³Department of Molecular and Clinical Cancer Medicine, University of Liverpool, Liverpool, Merseyside L69 3BX;

⁴Section of Experimental Haematology, Leeds Institute of Medical Research, University of Leeds, St. James's University Hospital, Leeds, Yorkshire LS9 7TF, UK

Received May 24, 2020; Accepted November 11, 2020

DOI: 10.3892/ol.2021.12524

Abstract. With its significant contribution to cancer mortality globally, advanced colorectal cancer (CRC) requires new treatment strategies. However, despite recent good results for mismatch repair (MMR)-deficient CRC and other malignancies, such as melanoma, the vast majority of MMR-proficient CRCs are resistant to checkpoint inhibitor (CKI) therapy. MMR-proficient CRCs commonly develop from precursor adenomas with enhanced Wnt-signalling due to adenomatous polyposis coli (*APC*) mutations. In melanomas with enhanced Wnt signalling due to stabilized β -catenin, immune anergy and resistance to CKI therapy has been observed, which is dependent on micro-environmental myelomonocytic (MM) cell depletion in melanoma models. However, MM populations of colorectal adenomas or CRC have not been studied.

To characterize resident intestinal MM cell populations during the early stages of tumorigenesis, the present study utilized the *Apc*^{Min/+} mouse as a model of MMR-proficient CRC, using enhanced green fluorescent protein (EGFP) expression in the mouse lysozyme (*M-lys*)^{lys-EGFP/+} mouse as a pan-myelomonocytic cell marker and a panel of murine macrophage surface markers. Total intestinal lamina propria mononuclear cell (LPMNC) numbers significantly decreased with age ($2.32 \pm 1.39 \times 10^7$ [n=4] at 33 days of age vs. $1.06 \pm 0.24 \times 10^7$ [n=8] at 109 days of age) during intestinal adenoma development in *Apc*^{Min/+} mice (P=0.05; unpaired Student's t-test), but not in wild-type littermates (P=0.35). Decreased total LPMNC numbers were associated with atrophy of intestinal lymphoid follicles and the absence of MM/lymphoid cell aggregates in *Apc*^{Min/+} mouse intestine, but not spleen, compared with wild-type mice. Furthermore, during the early stage of intestinal adenoma development, there was a two-fold reduction of *M-lys* expressing cells (P=0.05) and four-fold reduction of ER-HR3 (macrophage sub-set) expressing cells (P=0.05; two tailed Mann-Whitney U test) in mice with reduced total intestinal LPMNCs (n=3). Further studies are necessary to determine the relevance of these findings to immune-surveillance of colorectal adenomas or MMR-proficient CRC CKI therapy resistance.

Correspondence to: Dr Olusola O. Faluyi or Dr P. Louise Coletta, Section of Molecular Gastroenterology, Leeds Institute of Medical Research, University of Leeds, St. James's University Hospital, Beckett Street, Leeds, Yorkshire LS9 7TF, UK

E-mail: Olusola.Faluyi1@nhs.net

E-mail: P.L.Coletta@leeds.ac.uk

Abbreviations: *Apc*, adenomatous polyposis coli gene; CKI, checkpoint inhibitor; CRC, colorectal cancer; EGFP, enhanced green fluorescent protein; FAP, familial adenomatous polyposis; LPMNC, lamina propria mononuclear cell; Mac-mix, mixture of antibodies to macrophage markers (ER-HR3, F4/80 and MOMA-1); MSI, microsatellite instability; MMR, mismatch repair; MM, myelomonocytic; PD-1, programmed cell death protein-1; PGE2, prostaglandin E2; SEM, standard error of the mean; Treg, regulatory T lymphocyte; v/v, volume in total volume of solution; w/v, weight in total volume of solution

Key words: *Apc*, mouse lysozyme, *Apc*^{Min/+} mouse, myelomonocytic, intestine, tumorigenesis

Introduction

Colorectal cancer (CRC), which accounts for nearly a million global deaths each year, remains a major cause of cancer mortality due to the limited efficacy of currently available systemic treatment for advanced disease (1). Consequently, improved understanding of the disease is required to further optimize systemic treatment strategies including immunotherapy. CRC is known to develop from intestinal epithelium following progressive accumulation of genetic alterations, which include mutations of the adenomatous polyposis coli (*APC*) gene (2). In the highly evolutionary conserved canonical Wnt signalling pathway, APC is known to target β -catenin for cytoplasmic

degradation, thus preventing its nuclear translocation to promote tumorigenesis (3). Most sporadic CRCs are thought to acquire *APC* mutations as an early event during tumorigenesis, prior to the development of adenomas (4). Furthermore, patients with familial adenomatous polyposis (FAP) carry a germ-line *APC* mutation, which predisposes the individual to intestinal adenomas and CRC (5). The *Apc*^{Min/+} mouse is a model of FAP that possess a germline heterozygous $\Delta 850$ *Apc* mutation (6). Such mice develop predominantly small intestinal adenomas and die at ~ 130 days of age from the intestinal adenoma burden (6). In addition, haematopoietic defects, including the development of generalized atrophy of lymphoid tissue, occur during the early stages of intestinal tumorigenesis at ~ 80 days of age (7), while myeloid defects have been reported at an advanced age in the *Apc*^{Min/+} mouse and another mouse model that is haplo-insufficient for *Apc* (8,9).

Over the past decade, immune checkpoint inhibitor (CKI) therapy including targeting programmed cell death protein-1 (PD-1), has emerged as an effective therapeutic strategy against several types of cancer, such as lung, melanoma and renal cell cancer (10). More recently, CKI therapy has been shown to be effective for the mismatch repair (MMR)-deficient or microsatellite instability (MSI)-high subset of various malignancies, including CRC (11,12). However, this strategy has proven ineffective so far in the management of the majority of MMR-proficient CRC that represent $>90\%$ of sporadic CRCs (13). For melanoma, higher neoantigen burden (14) and a greater extent of T lymphocyte infiltration (15) are correlated with enhanced responses to PD-1 inhibition. However, T lymphocyte and MM cell infiltration have been inversely correlated with enhanced β -catenin pathway signalling in melanoma (16). Furthermore, a study in autochthonous mouse melanoma models with constitutive β -catenin signalling has demonstrated the dependence of T lymphocyte infiltration on the MM cell population (16). Therefore, characterization of the intestinal MM cell population during intestinal adenoma development in the *Apc*^{Min/+} model could yield insight into any early MM population changes associated with enhanced Wnt signalling.

A review on MM cells highlighted their heterogeneity, with no pan-MM cell marker defined, which has compounded previous studies on MM cell populations (17). However, a mouse with EGFP knocked into the mouse-lysozyme (*M-lys*) locus by homologous recombination (*M-lys*^{lys-EGFP/lys-EGFP}) was previously generated, which utilizes EGFP expression to facilitate studies on murine MM cells (18). In this model, EGFP fluorescence has been observed in multiple surface marker-defined peripheral MM sub-populations (18). The present study had two aims. First, to determine if there is reduction of the total resident intestinal LPMNC population during the early stage of intestinal tumorigenesis. Furthermore, utilizing *Apc*^{Min/+} and wild-type mice bred onto the *M-lys*^{lys-EGFP/+} background, it was investigated if there is a reduction in the resident intestinal MM cell population during the early stage of intestinal tumorigenesis.

Materials and methods

Mice. C57BL/6J and C57BL/6J-*Apc*^{Min/+} mice were obtained from The Jackson Laboratory. C57BL/6J/Sv129-*M-lys*^{lys-EGFP/lys-EGFP} mice (18) were obtained from Albert Einstein College of

Medicine. All mice were bred in-house, kept under isolator conditions at temperatures between 19 and 23°C on a 12-h light-dark cycle. They were pathogen-free by regular bacteriological and serological testing. Relative humidity was kept between 45 and 55%. The mice were fed on mouse complete maintenance diet with free access to food and water. For the experiments described here, the following mice were utilized: *Apc*^{+/+}*M-lys*^{+/+} (n=20), *Apc*^{Min/+}*M-lys*^{+/+} (n=23), *Apc*^{+/+}*M-lys*^{lys-EGFP/+} (n=9) and *Apc*^{Min/+}*M-lys*^{lys-EGFP/+} (n=12).

Mouse breeding and genotyping. *Apc*^{+/+} and *Apc*^{Min/+} mice on the *M-lys*^{lys+/+} background were obtained by mating male *Apc*^{Min/+}*M-lys*^{lys+/+} mice with female *Apc*^{+/+}*M-lys*^{lys+/+} mice. Furthermore, *Apc*^{Min/+} and *Apc*^{+/+} mice on the *M-lys*^{lys-EGFP/+} background were obtained by mating male *Apc*^{Min/+}*M-lys*^{lys+/+} mice with female *Apc*^{+/+}*M-lys*^{lys-EGFP/lys-EGFP} mice. The offspring were genotyped for *Apc* and *M-lys* at ~ 30 days of age by PCR analysis of genomic DNA (18,19).

Resident peritoneal cell, splenic and intestinal tissue collection. Each mouse was sacrificed between 30 and 138 days of age for experiments described below by cervical dislocation, immediately after which the peritoneal cavity was opened and peritoneal mononuclear cells (when required) were obtained by lavage with sterile phosphate buffer saline (PBS) at room temperature (25°C), prior to dissection of the spleen or whole intestine. Splenic and intestinal tissues were collected in ice cold PBS, then stored in ice cold PBS for ≤ 5 min until processed as described in subsequent sections.

Intestinal adenoma count. Following lavage for peritoneal cells and dissection of the spleen, intestine was removed from the pylorus to the anus. The small intestine was then separated from the caecum and colon. Intestines were flushed out gently with PBS until no luminal content remained, after which they were carefully cut and opened out longitudinally to avoid adenoma disruption. For five *Apc*^{Min/+}*M-lys*^{lys-EGFP/+} at 92 ± 23 days of age, adenomas were counted by naked eye examination of small intestinal tissue.

Histology. Tissue from the small intestine and spleen of three pairs of *Apc*^{+/+}*M-lys*^{lys-EGFP/+} and *Apc*^{Min/+}*M-lys*^{lys-EGFP/+} mice at 93 ± 23 days of age underwent histological evaluation and immunohistochemistry for EGFP localisation as described below. Tissue from an SW480 human CRC xenograft transfected with an EGFP-expressing herpes saimiri viral vector served as positive control due to previously demonstrated EGFP expression (20). Tissue from age matched *Apc*^{Min/+}*M-lys*^{lys+/+} mice served as negative control. Sections were fixed in 4% (w/v) paraformaldehyde in PBS for 6 h at 25°C and paraffin wax embedded. Sections were cut to 5-7- μ m thickness and underwent haematoxylin and eosin staining or immunohistochemistry (as described in the next section). Sections were viewed using fluorescence and phase contrast microscopy by a NIKON Eclipse E1000 fluorescence microscope (Nikon Corporation). Images were then captured using LUCIA GF imaging software (version 4.60) (Nikon Corporation).

Immunohistochemistry for the detection of EGFP. Steps of the procedure were performed at room temperature (25°C)

except otherwise stated. Sections were de-waxed progressively in xylene for 1 min each three times, then absolute (100%) ethanol for a minute each (x3), then washed in distilled water before endogenous tissue peroxidase activity was blocked by immersion of slides in 2% (v/v) H₂O₂ in absolute methanol for 15 min. Subsequently, slides were washed in distilled water for 10 min. Immunohistochemical staining of intestinal sections was carried out as previously described (21). Serum block was with 1.5% (v/v) goat serum (Dako; Agilent Technologies, Inc.) in PBS for 30 min. Sections were then incubated with rabbit anti-*Aquorea* anti-EGFP primary antibody (1:4,000; cat. no. A-6455; Invitrogen; Thermo Fisher Scientific, Inc.) for 20 h at 4°C, after which slides were washed in PBS four times for 5 min each. Sections were then incubated for 30 min with HRP/dextran polymer-conjugated goat anti-rabbit secondary antibody (ready to use; cat. no. K4002; Dako; Agilent Technologies, Inc.) at room temperature. Subsequently, sections were washed in PBS four times for 5 min each. Sections were then incubated for 10 min with 0.1% (v/v) diaminobenzidine solution [Dako; Agilent Technologies, Inc.] in Tris-buffer (0.05 M Tris (pH 7.6 with HCl)], containing 0.03% (v/v) H₂O₂ at room temperature. Sections were washed in tap water four times for 5 min each, counterstained with Mayer's Haematoxylin (cat no. MHS32; Sigma-Aldrich; Merck KGaA) for 90 sec at room temperature, followed by immersion in Scott's tap water (0.167 M and MgSO₄ and 0.042 M NaHCO₃ in distilled water) for 1 min. Slides were then rinsed in distilled water and the stained sections were dehydrated by immersion in absolute ethanol for 3 min three times, then immersed in xylene for three times 3 min each followed by mounting in DPX mountant (cat. no. 100579; Millipore Sigma). Sections were, viewed and images were captured as aforementioned.

Isolation and enumeration of small intestinal lamina propria mononuclear cells. Utilizing *Apc^{+/+} M-Lys^{+/+}* mice as controls, intestinal LPMNCs were isolated from *Apc^{Min/+} M-Lys^{+/+}* mice at the following ages: Weaning (~30 days of age; n=4 pairs), prior to the appearance of macroscopically visible adenomas (~70 days of age; n=8 pairs), prior to death from macroscopic adenoma burden (~100 days of age; n=8 pairs). LPMNCs were isolated from mouse small intestine at room temperature (25°C) with viability and numbers determined as previously described (22,23) ensuring complete enzymatic digestion of the intestines of mice at different ages.

Flow cytometric analysis of small intestinal lamina propria mononuclear cells. Flow cytometric analysis of small intestinal LPMNCs has been described previously for EGFP, phycoerythrin (PE) and propidium iodide (PI) expression (23). Flow cytometry was performed at room temperature (25°C) on intestinal LPMNCs of six *Apc^{+/+} M-Lys^{lys-EGFP/+}* mice and seven *Apc^{Min/+} M-Lys^{lys-EGFP/+}* mice at 74±2 days of age. Monoclonal primary antibodies utilized were as follows: F4/80 (1:100; cat. no. MCA497G; clone A3-1; BioRad Laboratories, Inc.), BMDM-1, ER-HR3 (1:10), ER-MP23, ER-MP58, ER-TR9, MOMA-1 (all 1:10) and MOMA-2. Antibodies (with the exclusion of F4/80) were hybridoma-conditioned supernatant, a kind gift from Professor Pieter Leenen (24). A PE-conjugated goat anti-rat antibody was utilized (cat no. 305009; Bio-Rad Laboratories, Inc.) at 1: 100 dilution. Cells were then washed

in 10% foetal calf serum (FCS) labelled with propidium iodide (cat. no. P4864; Sigma-Aldrich; Merck KGaA) at 1:2000 dilution. Flow cytometry was performed using 5x10⁴ LPMNCs and a FACS Vantage cytometer (Becton-Dickinson and Company) with Cell Quest™ software version 3.3 (Becton-Dickinson and Company). The R1 gate was set up to exclude PI-positive cells and cells with low forward scatter (deemed non-viable). EGFP-positive cells (fluorescence level greater than that obtained by <0.1% of wild-type LPMNCs) and macrophage marker positive cells ([M] with fluorescence level greater than that obtained by <0.1% of cells with non-specific labelling by control rat IgG) were analysed as expressing the relevant marker. Some cells were labelled with a cocktail of ER-HR3, F4/80 and MOMA-1 primary antibodies defined as the 'Mac-mix' (at the same concentration as utilized for single markers). BMDM-1, ER-MP23, ER-MP58, ER-TR9 and MOMA-2 were not evaluated further, due to the level of expression of undiluted hybridoma supernatant being no higher than for control rat IgG (data not shown).

Isolation of resident peritoneal cells. Lavaged peritoneal cells from three pairs of *Apc^{+/+} M-Lys^{lys-EGFP/+}* and *Apc^{Min/+} M-Lys^{lys-EGFP/+}* mice at 93±23 days were treated with 5 mM EDTA in Hank's Balanced Salt Solution (Invitrogen; Thermo Fisher Scientific, Inc.) for 75 min and collagenase/dispase enzymes for 90 min at 37°C as for small intestinal LPMNCs (23). Peritoneal cells were then washed twice in an excess of 10% (v/v) foetal calf serum in PBS and re-suspended at 25°C in the same culture medium as for LPMNCs prior to been viewed by fluorescence microscopy.

Statistical analysis. The mean ± standard error of mean (SEM) was calculated for numbers or proportions of cells belonging to different small intestinal LPMNC sub-populations of different groups of mice. Analysis of the difference between total LPMNCs of the oldest and youngest mice of either genotype (parametric data) was compared using unpaired two-tailed Student's t-tests. Statistical comparison of the myelomonocytic sub-population and adenoma numbers between mice was conducted using two-tailed Mann-Whitney U tests. Statistical analysis utilized Minitab software version 13 (Minitab, LLC). P≤0.05 was considered to indicate a statistically significant difference.

Results

Small intestinal LPMNC numbers decrease with age in *Apc^{Min/+}* mice. Initially, the total small intestinal LPMNC population was characterised during intestinal tumorigenesis in the *Apc^{Min/+}* mouse. It was determined if there were any differences in small intestinal LPMNC numbers with age. There were no significant differences in LPMNC viability between groups of mice (Table I). There was no significant difference in total intestinal LPMNC numbers with age in *Apc^{+/+}* mice (33±1 vs. 109±2 days old; P=0.35), though older mice had a trend to reduced total LPMNCs (Table I). By contrast, total intestinal LPMNCs numbers significantly reduced with age in *Apc^{Min/+}* mice (33±1 vs. 109±2 days old; P=0.05; Table I). This suggested significantly reduced intestinal LPMNCs with age in *Apc^{Min/+}* mice.

Table I. Decreased numbers of small intestinal LPMNCs with age in *Apc*^{Min/+} mice.

Age, (days)	Mouse strain			
	<i>Apc</i> ^{+/+}		<i>Apc</i> ^{Min/+}	
	LPMNCs, x10 ⁶	Viability, %	LPMNCs, x10 ⁶	Viability, %
33±1	25.0±6.0	81.5±2.1	23.2±13.9	81.3±4.3
71±1	17.1±2.6	78.2±1.9	12.3±2.4	77.1±2.4
109±2	18.7±3.3 ^a	76.8±1.6	10.6±2.4 ^b	76.1±1.5

^aP=0.35 vs. *Apc*^{+/+} mice at 33±1 days of age; ^bP=0.05 vs. *Apc*^{Min/+} mice at 33±1 days of age.

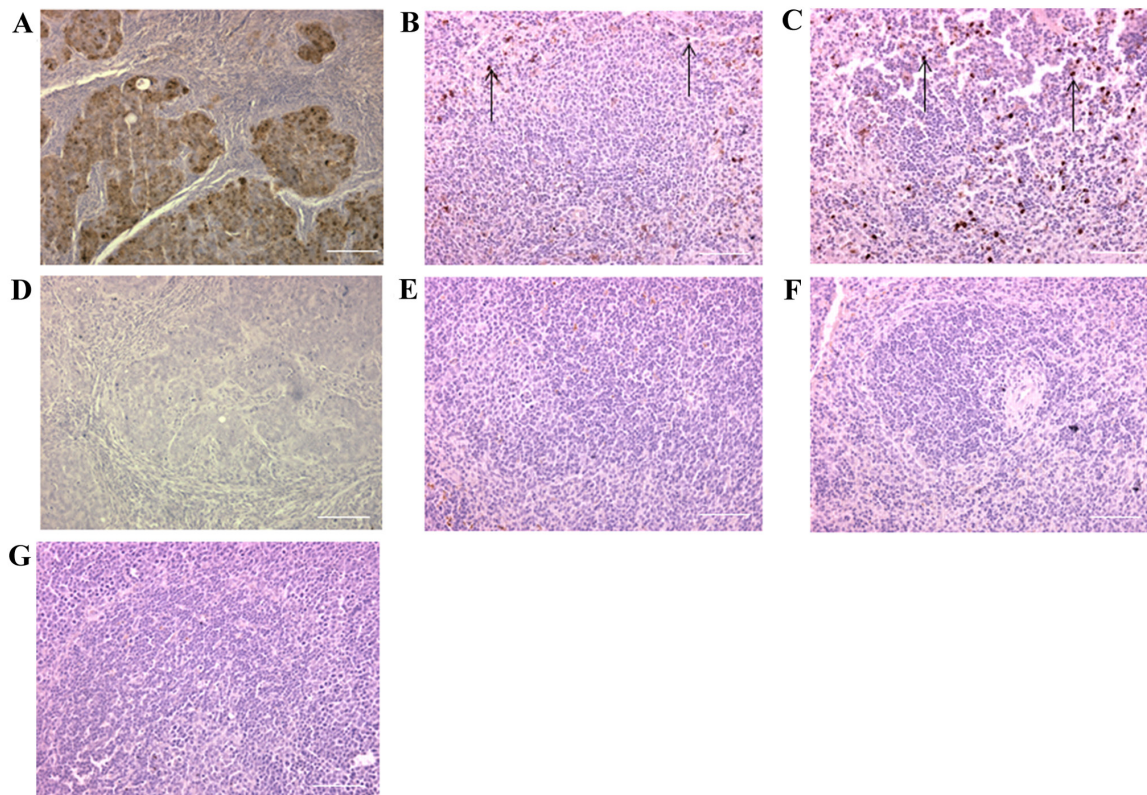


Figure 1. Localisation of EGFP expression in *Apc*^{+/+} *M-Lys*^{lys-EGFP/+} and *Apc*^{Min/+} *M-Lys*^{lys-EGFP/+} mouse spleen. Sections of the spleen of an *Apc*^{+/+} *M-Lys*^{lys-EGFP/+} mouse and an age-matched *Apc*^{Min/+} *M-Lys*^{lys-EGFP/+} mouse at 138 days of age were labelled with an antibody to EGFP (brown cells). Brown staining in (A) an EGFP-expressing SW480 cell line, (B) the spleen of an *Apc*^{+/+} *M-Lys*^{lys-EGFP/+} mouse and (C) the spleen of an *Apc*^{Min/+} *M-Lys*^{lys-EGFP/+} mouse. In sections with omission of the primary antibody, absence of brown staining in (D) EGFP-expressing SW480 cell line, (E) the spleen of an *Apc*^{+/+} *M-Lys*^{lys-EGFP/+} mouse and (F) the spleen of an *Apc*^{Min/+} *M-Lys*^{lys-EGFP/+} mouse. (G) Absence of brown staining in a section from the spleen of an *Apc*^{Min/+} *M-Lys*^{+/+} mouse. Arrows point to EGFP-expressing cells. Scale bars, 100 μ m. APC, adenomatous polyposis coli; EGFP, enhanced green fluorescent protein; M-lys, mouse lysozyme.

No significant effect of *M-lys* hemizyosity on *Apc*^{Min/+} mouse small intestinal tumorigenesis. A previous study reported no difference in the proportion of EGFP-expressing cells in the blood and bone marrow of *Apc*^{+/+} *M-Lys*^{lys-EGFP/lys-EGFP} compared with *Apc*^{+/+} *M-Lys*^{lys-EGFP/+} mice (18). Therefore, *Apc*^{+/+} and *Apc*^{Min/+} mice were bred onto the *M-Lys*^{lys-EGFP/+} background to facilitate the study of MM cell populations with intact *M-Lys* function. It was determined if there was any impact of heterozygous *M-Lys* deletion on intestinal tumorigenesis by counting macroscopic adenomas from *Apc*^{Min/+} *M-Lys*^{lys-EGFP/+} intestine. Adenoma numbers were 45.8±10 (mean ± SEM; n=5) from the small intestine of *Apc*^{Min/+} *M-Lys*^{lys-EGFP/+} mice (data not shown), similar

to that of *Apc*^{Min/+} *M-Lys*^{+/+} mice previously bred in our facility that had 53±4 tumours (mean ± SEM; n=25) (25). Consequently, hemizygous deletion of *M-Lys* appeared not to have significant impact on intestinal tumorigenesis in the *Apc*^{Min/+} mouse.

EGFP fluorescence in isolated small intestinal LPMNCs of M-Lys^{lys-EGFP/+} mice. *M-Lys* mRNA expression has previously been demonstrated in mouse intestine (26). The presence of EGFP protein was tested for and fluorescence in isolated intestinal LPMNCs of *M-Lys*^{lys-EGFP/+} mice. EGFP fluorescence in intestinal LPMNCs of *Apc*^{+/+} *M-Lys*^{lys-EGFP/+} mice in situ as well as in the LPMNC isolate was observed (Fig. S1).

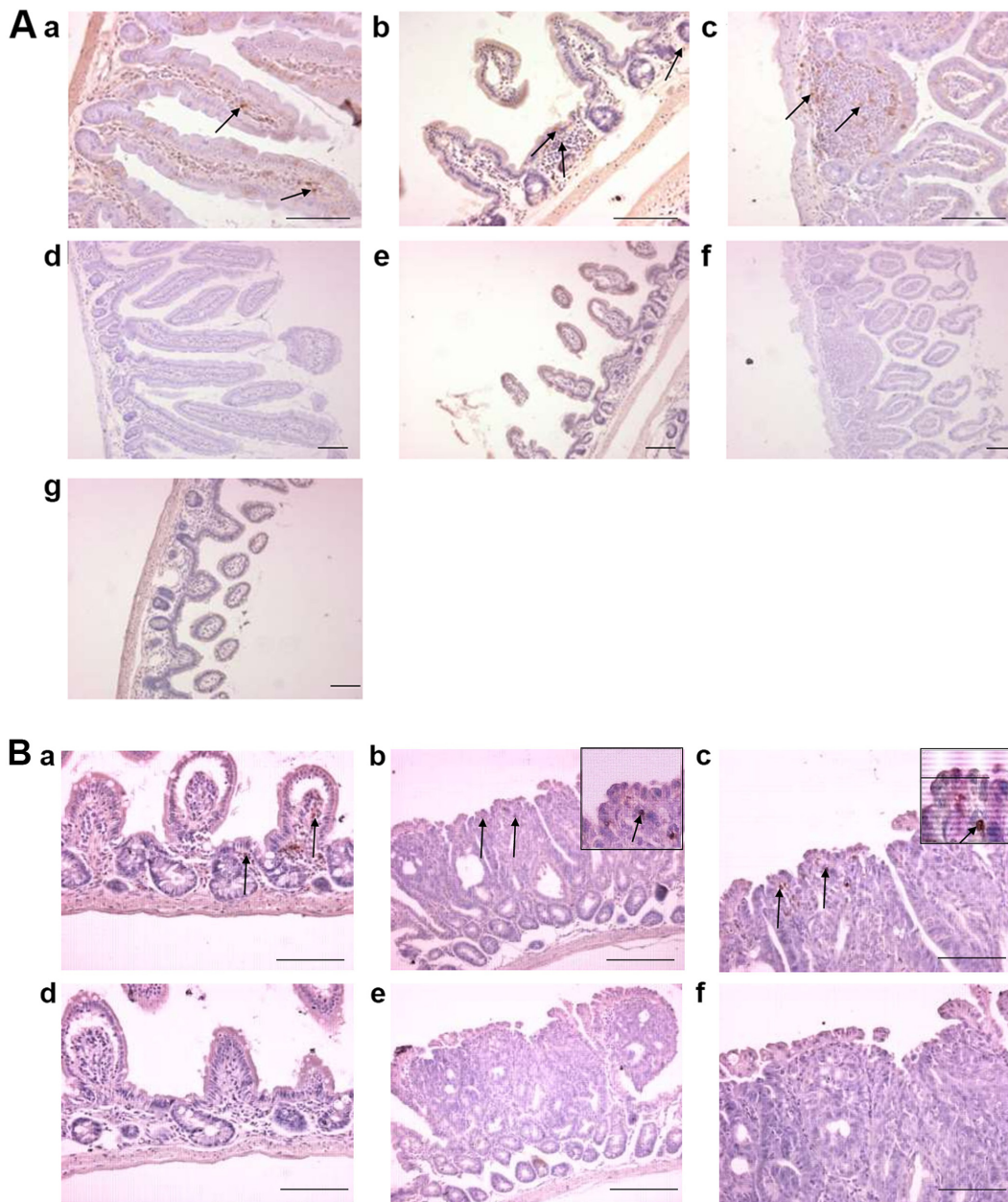


Figure 2. Localisation of EGFP expressing cells in $Apc^{+/+} M-Lys^{lys-EGFP/+}$ mouse small intestine. (A) Sections of the small intestine of an $Apc^{+/+} M-Lys^{lys-EGFP/+}$ mouse at 138 days of age labelled with an antibody to EGFP (brown cells). With the primary antibody to EGFP, brown staining in (a) proximal small intestine of the $Apc^{+/+} M-Lys^{lys-EGFP/+}$ mouse, (b) distal small intestine of the $Apc^{+/+} M-Lys^{lys-EGFP/+}$ mouse and (c) an intestinal lymphoid follicle of the distal small intestine of an $Apc^{+/+} M-Lys^{lys-EGFP/+}$ mouse (higher magnification, x600). In sections with omission of the primary antibody, absence of brown staining in (d) proximal small intestine and (e and f) distal small intestine of an $Apc^{+/+} M-Lys^{lys-EGFP/+}$ mouse stained with the EGFP antibody. (B) Sections of the distal small intestine of an $Apc^{Min/+} M-Lys^{lys-EGFP/+}$ mouse labelled with an antibody to EGFP. With the primary antibody to EGFP, brown staining in (a) LPMNCs within the villi and lamina propria of an $Apc^{Min/+} M-Lys^{lys-EGFP/+}$ mouse, (b and c) LPMNCs within an intestinal adenoma of an $Apc^{Min/+} M-Lys^{lys-EGFP/+}$ mouse. Inset are EGFP-expressing cells within intestinal adenomas, shown at higher magnification (magnification, x600). In sections with omission of the primary antibody, absence of brown staining in (d) distal small intestine and (e and f) adenomas. Arrows point to EGFP-expressing cells. Scale bars, 100 μ m. APC, adenomatous polyposis coli; EGFP, enhanced green fluorescent protein; LPMNCs, lamina propria mononuclear cells; M-Lys, mouse lysozyme.

EGFP expression in the spleen and small intestine of $Apc^{+/+} M-Lys^{lys-EGFP/+}$ and $Apc^{Min/+} M-Lys^{lys-EGFP/+}$ mice. Utilizing an EGFP-expressing SW480 human CRC xenograft as positive control, it was determined if there was any difference in the resident intestinal MM cell localization between $Apc^{+/+} M-Lys^{lys-EGFP/+}$ and $Apc^{Min/+} M-Lys^{lys-EGFP/+}$ mice at ~100 days of age (n=3 pairs) by immunohistochemistry for EGFP (Figs. 1 and 2). The spleen was studied as independent lymphoid tissue with a sentinel MM cell population. Even though there was some fibrotic distortion of $Apc^{Min/+} M-Lys^{lys-EGFP/+}$ splenic tissue, EGFP-expressing cells

were localized to the marginal zone of the spleen in both types of mice (Fig. 1B and C). In the intestine, EGFP-expressing cells were localized to intestinal villi and in particular lymphoid follicles of $Apc^{+/+} M-Lys^{lys-EGFP/+}$ mice (Fig. 2Aa-c). While EGFP-expressing cells were also localized to the intestinal villi of $Apc^{Min/+} M-Lys^{lys-EGFP/+}$ mice and the periphery of adenomas, lymphoid follicles were absent from the intestine of $Apc^{Min/+} M-Lys^{lys-EGFP/+}$ mice (Fig. 2Ba-c). This suggested loss of myelomonocytic cells and immune cell aggregates in $Apc^{Min/+} M-Lys^{lys-EGFP/+}$ mouse intestine

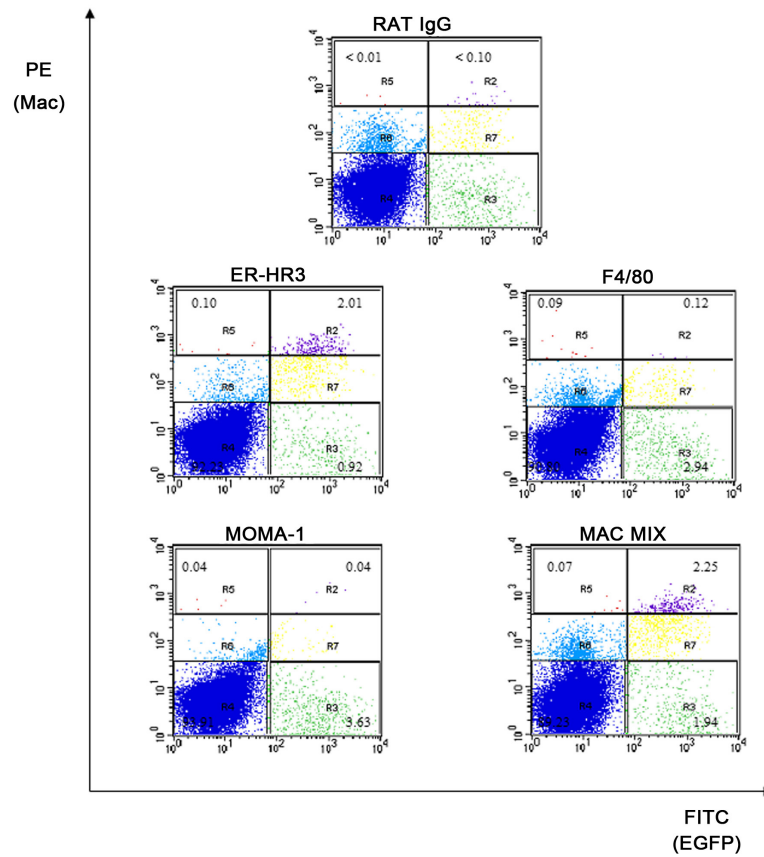


Figure 3. Macrophage marker flow cytometry on *M-Lys^{lys-EGFP/+}* intestinal LPMNCs. Representative flow cytometry plots from *Apc^{+/+}* *M-Lys^{lys-EGFP/+}* mouse intestinal LPMNCs. Figures show the percentage of the total population of LPMNCs in relevant regions. EGFP fluorescence is on the abscissa, while PE fluorescence for macrophage markers is on the ordinate. R1, viable cell gate (not shown); R2, G+M+; R3, G-M-; R4, G-M-; R5, G-M+; R6, LPMNCs that do not express EGFP, but were labelled by the macrophage surface marker at a similar level to non-specific rat IgG; R7, LPMNCs that expressed EGFP and were labelled by macrophage surface markers at a similar level to non-specific rat IgG. LPMNCs, lamina propria mononuclear cells; M-lys, mouse lysozyme; PE, phycoerythrin; G+, EGFP-positive LPMNCs, G-: EGFP-negative LPMNCs. M+, LPMNCs labelled by macrophage markers above levels of non-specific binding by rat IgG. M-, LPMNCs not labelled by macrophage markers

Table II. Small intestinal myelomonocytic cell populations of *Apc^{Min/+}* *M-Lys^{lys-EGFP/+}* and *Apc^{+/+}* *M-Lys^{lys-EGFP/+}* mice at 74±2 days of age.

Myelomonocytic cell marker	<i>Apc^{+/+}</i>	<i>Apc^{Min/+}</i>	P-value
EGFP (M-lys)	4.29±0.68	2.90±0.47	0.11
ERHR-3			
G-	0.11±0.03	0.13±0.04	0.83
G+	1.02±0.25	0.55±0.13	0.23
F4/80			
G-	0.22±0.17	0.31±0.18	0.52
G+	0.24±0.10	0.14±0.07	0.20
MOMA-1			
G-	0.04±0.01	0.07±0.02	0.12
G+	0.13±0.09	0.04±0.01	0.39
MAC-MIX			
G-	0.16±0.10	0.15±0.05	0.48
G+	1.20±0.34	0.66±0.18	0.28

Pre-immune rat IgG served as the antibody-isotype control. G+, EGFP-positive LPMNCs; G, EGFP-negative LPMNCs.

*Small intestinal myelomonocytic sub-populations of *Apc^{+/+}* *M-Lys^{lys-EGFP/+}* and *Apc^{Min/+}* *M-Lys^{lys-EGFP/+}* mice.* To determine any differences in the intestinal MM population during the early stages of intestinal tumorigenesis, mice were studied at ~70 days of age, which is prior to overt *Apc^{Min/+}* mouse lymphoid atrophy (7). This was also prior to ulceration, bleeding and potential secondary inflammation associated with advanced intestinal adenomas (6). As for mice on the *M-Lys^{+/+}* background, there was a trend towards reduced total intestinal LPMNCs in *Apc^{Min/+}* *M-Lys^{lys-EGFP/+}* mice which did not reach statistical significance ($2.65 \pm 0.23 \times 10^7$ *Apc^{+/+}* *M-Lys^{lys-EGFP/+}* vs. $1.72 \pm 0.39 \times 10^7$ *Apc^{Min/+}* *M-Lys^{lys-EGFP/+}* mice, $P=0.12$) Typical flow cytometry plots are shown in Fig. 3. There was no significant difference in the proportion of cells in the R1 gate ([%] *Apc^{+/+}* 35.40 ± 4.00 vs *Apc^{Min/+}* 38.00 ± 4.60 , $P=0.52$). Data on the three expressed macrophage marker antibodies, their mixture (Mac mix) and EGFP are displayed for *Apc^{+/+}* *M-Lys^{lys-EGFP/+}* and *Apc^{Min/+}* *M-Lys^{lys-EGFP/+}* mice (Table II). A higher proportion of LPMNCs from *Apc^{+/+}* *M-Lys^{lys-EGFP/+}* mice ($n=6$) expressed EGFP ($P=0.11$), ER-HR3 ($P=0.11$) or the Mac mix ($P=0.18$) compared with *Apc^{Min/+}* *M-Lys^{lys-EGFP/+}* littermates ($n=7$) (Table II). However, these differences were not statistically significant.

*Lower numbers of small intestinal myelomonocytic cells in the *Apc^{Min/+}* *M-Lys^{lys-EGFP/+}* mice with the lowest total small*

intestinal LPMNC numbers. To clarify if there was an association between the trend to reduced *Apc^{Min/+}* total intestinal LPMNC and MM cell numbers, the lamina propria MM cell population of mice with the lowest total LPMNC yield were studied (*Apc^{Min/+}M-Lys^{lys-EGFP/+}*; mice nos. 4, 5 and 7; Tables SI and SII). These three mice had an LPMNC yield <35% compared with the average LPMNC yield of *Apc^{+/+}* mice. For these three *Apc^{Min/+}M-Lys^{lys-EGFP/+}* mice, the proportion of EGFP-expressing cells (1.78 ± 0.26) was >2-fold depleted compared with the mean for *Apc^{+/+}* mice ($P=0.05$) while the proportion of Mac-mix expressing cells (0.37 ± 0.04) was ~4-fold depleted compared with the mean for *Apc^{+/+}* mice ($P=0.05$). This suggested that there was depletion of the myelomonocytic sub-population associated with reduced intestinal LPMNCs.

Discussion

Selective EGFP fluorescence of MM cells without significant impact on tumorigenesis in the novel *Apc^{Min/+}M-Lys^{lys-EGFP/+}* mouse in the present study prompted investigation into the MM cell population. No pan-myelomonocytic cell marker has yet been fully validated for the murine MM cell population, which the present observation of EGFP-negative Mac mix expressing cells corroborates. While a range of myelomonocytic cell markers were used in the present study, rare subsets not evaluated in the present study should not be ignored. However, the murine *M-lys*-expressing MM sub-population has been ascribed roles in phagocytosis and antigen presentation in the intestinal micro-environment, which are crucial to the immune response (27). A notable observation of the current study was a reduction in the *Apc^{Min/+}* lamina propria MM cell population early during intestinal adenoma development, associated with loss of intestinal lymphoid/MM cell aggregates but with retention of splenic marginal zone MM cells. It is possible that similar to the reduction in total intestinal LPMNC numbers observed, MM cell depletion is progressive through adenoma development. Conventional dendritic cells that function as antigen presenting cells in the intestinal micro-environment are known to reside in intestinal lymphoid follicles (28). Consequently, the loss of lymphoid/MM cell interaction during intestinal adenoma development could impair the development of an immune response to tumour antigens, as previously shown in an autochthonous melanoma model (16), thus compromising immunosurveillance to prevent adenoma growth. In this respect, the prognosis following resection of early CRC is positively correlated with the extent of intra-tumoral lymphocytic infiltration (29). Furthermore, response to PD-1-inhibition in melanoma is associated with the presence of a primed peri-tumoral cytotoxic lymphocyte population (15).

Apc^{Min/+} mice ≤ 84 days of age did not have evidence of reduced peripheral MM cells or lymphocytes (8). Consequently, total intestinal lamina propria and intestinal MM cell depletion in 70-day old *Apc^{Min/+}* mice appeared to be due to factors in the intestinal micro-environment. After weaning in mice, F4/80-positive resident intestinal macrophages of embryonic origin are now known to be replaced by F4/80-negative macrophages, which are constantly re-populated from the peripheral circulation and adopt an anti-inflammatory phenotype in the

intestinal microenvironment (30,31). We previously demonstrated that the resident intestinal MM population is the highest PGE2-secreting intestinal LPMNC sub-population in mice. Furthermore, there is a trend for higher PGE2 production by the *Apc^{Min/+}* mouse resident intestinal MM population compared with the *Apc^{+/+}* mouse (23). PGE2 has previously been ascribed an immunosuppressive role (32,33), which would be consistent with an anti-inflammatory MM cell phenotype. It is noteworthy that MM cell conversion to an immunosuppressive phenotype has been shown to take up to 96 h after MM cell migration into the intestinal micro-environment; with dendritic cells typically surviving for several days while macrophages typically survive for several weeks (28,34). Consequently, in this respect, enhanced Wnt signalling may be physiologically relevant to signal exclusion of MM cells prior to their conversion to an immunosuppressive phenotype in the *Apc^{Min/+}* intestinal milieu. However, other factors, such as cyclooxygenase-2 (35), TGF- β and T regulatory cells (36) may play a role in MM cell depletion from the intestinal micro-environment.

Out of the murine macrophage surface markers evaluated in the present study, ER-HR3 was the most widely expressed by intestinal lamina propria macrophages, irrespective of *Apc* genotype. ER-HR3 is known to be expressed by a sub-set of peripheral and resident tissue macrophages including those in sentinels, such as the skin, spleen and lymph nodes (37). Functionally, ER-HR3-expressing macrophages have been shown to be phagocytic and associated with immune latent milieu, such as the granulomata of BCG infected mice and with the relative exclusion of F4/80-expressing macrophages, which are more common in other murine tissue (38).

In conclusion, the present study demonstrated that the loss of MM/lymphoid interaction occurs during the early stages of *Apc^{Min/+}* intestinal tumorigenesis, which may be due to enhanced micro-environmental Wnt signalling. Subsequent anergy to emerging tumour neoantigens could compromise tumour immunosurveillance in the *Apc^{Min/+}* model. The relevance of this to colorectal adenomas and cancer requires evaluation, as well as the possibility that, similar to advanced melanoma, immune changes secondary to enhanced Wnt signalling may persist in MMR-proficient CRC. Furthermore, the mechanism to MM cell depletion requires further evaluation. Such studies may contribute to understanding the resistance to CKI therapy of MMR-proficient CRC despite a tendency for higher neoantigen burden compared with other malignancies, such as renal or bladder cancer (14).

Acknowledgements

The authors would like to thank Dr Sarah Holwell and Mr David Brooke (University of Leeds) who assisted with mouse genotyping, Dr Peter Smith, Ms Deborah Clarke and Ms Liz Straszynski (University of Leeds) for help with EGFP-expressing SW480 colorectal cell line tissue, L-cell conditioned medium and flow cytometric analysis, respectively, Professor Thomas Graf (Albert Einstein College of Medicine) for supplying C57BL/6J/Sv129-*M-Lys^{lys-EGFP/lys-EGFP}* mice and Professor Pieter Leenen (Erasmus University) for providing hybridoma supernatant antibodies to murine macrophage surface markers. The abstract was presented 4th-6th

November 2018 at the UK Annual National Cancer Research Institute conference in Glasgow, UK.

Funding

OOF was funded by an Overseas Research Student Scholarship. Work on intestinal tumorigenesis at St. James's University Hospital was funded by Yorkshire Cancer Research (grant no. L283).

Availability of data and materials

The datasets generated and/or analysed during the current study are available from the corresponding author on reasonable request.

Authors' contributions

OOF performed experiments and wrote the initial version of the manuscript. OOF, MAH, AFM, CB and PLC were involved in study design, interpretation of the data and statistical analysis. All authors confirm authenticity of the data and agreed to the final version of the manuscript.

Ethics approval and consent to participate

All animal work was carried out under the Animals (Scientific Procedures) Act 1986 (PPL 40/3291 UK Home Office). Ethical approval to conduct the study was obtained from The University of Leeds Animal Welfare and Ethical Review Committee.

Patient consent for publication

Not applicable.

Competing interests

The authors declare that they have no competing interests.

References

- Arnold M, Sierra MS, Laversanne M, Soerjomataram I, Jemal A and Bray F: Global patterns and trends in colorectal cancer incidence and mortality. *Gut* 66: 683-691, 2017.
- Fearon ER and Vogelstein B: A genetic model for colorectal tumorigenesis. *Cell* 61: 759-767, 1990.
- Moon RT, Bowerman B, Boutros M and Perrimon N: The promise and perils of Wnt signaling through beta-catenin. *Science* 296: 1644-1646, 2002.
- Ashton-Rickardt PG, Dunlop MG, Nakamura Y, Morris RG, Purdie CA, Steel CM, Evans HJ, Bird CC and Wyllie AH: High frequency of APC loss in sporadic colorectal carcinoma due to breaks clustered in 5q21-22. *Oncogene* 4: 1169-1174, 1989.
- Nishisho I, Nakamura Y, Miyoshi Y, Miki Y, Ando H, Horii A, Koyama K, Utsunomiya J, Baba S and Hedge P: Mutations of chromosome 5q21 genes in FAP and colorectal cancer patients. *Science* 253: 665-669, 1991.
- Moser AR, Pitot HC and Dove WF: A dominant mutation that predisposes to multiple intestinal neoplasia in the mouse. *Science* 247: 322-324, 1990.
- Coletta PL, Müller AM, Jones EA, Mühl B, Holwell S, Clarke D, Meade JL, Cook GP, Hawcroft G, Ponchel F, *et al*: Lymphodepletion in the *Apc^{Min/+}* mouse model of intestinal tumorigenesis. *Blood* 103: 1050-1058, 2004.
- Lane SW, Sykes SM, Al-Shahrour F, Shterental S, Paktinat M, Lo Celso C, Jesneck JL, Ebert BL, Williams DA and Gilliland DG: The *Apc(min)* mouse has altered hematopoietic stem cell function and provides a model for MPD/MDS. *Blood* 115: 3489-3497, 2010.
- Wang J, Fernald AA, Anastasi J, Le Beau MM and Qian Z: Haploinsufficiency of *Apc* leads to ineffective hematopoiesis. *Blood* 115: 3481-3488, 2010.
- Topalian SL, Hodi FS, Brahmer JR, Gettinger SN, Smith DC, McDermott DF, Powderly JD, Carvajal RD, Sosman JA, Atkins MB, *et al*: Safety, activity, and immune correlates of anti-PD-1 antibody in cancer. *N Engl J Med* 366: 2443-2454, 2012.
- Marabelle A, Le DT, Ascierto PA, Di Giacomo AM, De Jesus-Acosta A, Delord JP, Geva R, Gottfried M, Penel N, Hansen AR, *et al*: Efficacy of pembrolizumab in patients with noncolorectal high microsatellite instability/mismatch repair-deficient cancer: Results from the phase II KEYNOTE-158 study. *J Clin Oncol* 38: 1-10, 2020.
- Overman MJ, Lonardi S, Wong KYM, Lenz HJ, Gelsomino F, Aglietta M, Morse MA, Van Cutsem E, McDermott R, Hill A, *et al*: Durable clinical benefit with nivolumab plus ipilimumab in DNA mismatch repair-deficient/microsatellite instability-high metastatic colorectal cancer. *J Clin Oncol* 36: 773-779, 2018.
- Toh JWT, de Souza P, Lim SH, Singh P, Chua W, Ng W and Spring KJ: The potential value of immunotherapy in colorectal cancers: Review of the evidence for programmed death-1 inhibitor therapy. *Clin Colorectal Cancer* 15: 285-291, 2016.
- Schumacher TN and Schreiber RD: Neoantigens in cancer immunotherapy. *Science* 348: 69-74, 2015.
- Tumeh PC, Harview CL, Yearley JH, Shintaku IP, Taylor EJ, Robert L, Chmielowski B, Spasic M, Henry G, Ciobanu V, *et al*: PD-1 blockade induces responses by inhibiting adaptive immune resistance. *Nature* 515: 568-571, 2014.
- Spranger S, Bao R and Gajewski TF: Melanoma-intrinsic β -catenin signalling prevents anti-tumour immunity. *Nature* 523: 231-235, 2015.
- Bain CC and Mowat AM: Macrophages in intestinal homeostasis and inflammation. *Immunol Rev* 260: 102-117, 2014.
- Faust N, Varas F, Kelly LM, Heck S and Graf T: Insertion of enhanced green fluorescent protein into the lysozyme gene creates mice with green fluorescent granulocytes and macrophages. *Blood* 96: 719-726, 2000.
- Dietrich WF, Lander ES, Smith JS, Moser AR, Gould KA, Luongo C, Borenstein N and Dove W: Genetic identification of *Mom-1*, a major modifier locus affecting *Min*-induced intestinal neoplasia in the mouse. *Cell* 75: 631-639, 1993.
- Smith PG, Coletta PL, Markham AF and Whitehouse A: In vivo episomal maintenance of a herpesvirus saimiri-based gene delivery vector. *Gene Ther* 8: 1762-1769, 2001.
- Walter I, Fleischmann M, Klein D, Müller M, Salmons B, Günzburg WH, Renner M and Gelbmann W: Rapid and sensitive detection of enhanced green fluorescent protein expression in paraffin sections by confocal laser scanning microscopy. *Histochem J* 32: 99-103, 2000.
- Newberry RD, Stenson WF and Lorenz RG: Cyclooxygenase-2-dependent arachidonic acid metabolites are essential modulators of the intestinal immune response to dietary antigen. *Nat Med* 5: 900-906, 1999.
- Hull MA, Faluyi OO, Ko CW, Holwell S, Scott DJ, Cuthbert RJ, Poulosom R, Goodlad R, Bonifer C, Markham AF, *et al*: Regulation of stromal cell cyclooxygenase-2 in the *Apc^{Min/+}* mouse model of intestinal tumorigenesis. *Carcinogenesis* 27: 382-391, 2006.
- Leenen PJ, de Bruijn MF, Voerman JS, Campbell PA and van Ewijk W: Markers of mouse macrophage development detected by monoclonal antibodies. *J Immunol Methods* 174: 5-19, 1994.
- Scott DJ, Hull MA, Cartwright EJ, Lam WK, Tisbury A, Poulosom R, Markham AF, Bonifer C and Coletta PL: Lack of inducible nitric oxide synthase promotes intestinal tumorigenesis in the *Apc(Min/+)* mouse. *Gastroenterology* 121: 889-899, 2001.
- Keshav S, Chung P, Milon G and Gordon S: Lysozyme is an inducible marker of macrophage activation in murine tissues as demonstrated by in situ hybridization. *J Exp Med* 174: 1049-1058, 1991.
- Lelouard H, Fallet M, de Bovis B, Méresse S and Gorvel JP: Peyer's patch dendritic cells sample antigens by extending dendrites through M cell-specific transcellular pores. *Gastroenterology* 142: 592-601.e3, 2012.
- Joeris T, Müller-Luda K, Agace WW and Mowat AM: Diversity and functions of intestinal mononuclear phagocytes. *Mucosal Immunol* 10: 845-864, 2017.

29. Emile JF, Julié C, Le Malicot K, Lepage C, Tabernero J, Mini E, Folprecht G, Van Laethem JL, Dimet S, Boulagnon-Rombi C, *et al*: PETACC8 Study Investigators; Austrian Breast and Colorectal cancer Study Group (ABCSCG); Belgian Group of Digestive Oncology (BGDO); John Allen Bridgewater: Prospective validation of a lymphocyte infiltration prognostic test in stage III colon cancer patients treated with adjuvant FOLFOX. *Eur J Cancer* 82: 16-24, 2017.
30. Bain CC, Bravo-Blas A, Scott CL, Perdiguero EG, Geissmann F, Henri S, Malissen B, Osborne LC, Artis D and Mowat AI: Constant replenishment from circulating monocytes maintains the macrophage pool in the intestine of adult mice. *Nat Immunol* 15: 929-937, 2014.
31. Shaw TN, Houston SA, Wemyss K, Bridgeman HM, Barbera TA, Zangerle-Murray T, Strangward P, Ridley AJL, Wang P, Tamoutounour S, *et al*: Tissue-resident macrophages in the intestine are long lived and defined by Tim-4 and CD4 expression. *J Exp Med* 215: 1507-1518, 2018.
32. Wang D and DuBois RN: The Role of Prostaglandin E(2) in Tumor-Associated Immunosuppression. *Trends Mol Med* 22: 1-3, 2016.
33. Faluyi OO, Fitch P and Howie SE: An increased CD25-positive intestinal regulatory T lymphocyte population is dependent upon Cox-2 activity in the *Apc^{min/+}* model. *Clin Exp Immunol* 191: 32-41, 2018.
34. Bain CC, Scott CL, Uronen-Hansson H, Gudjonsson S, Jansson O, Grip O, Williams M, Malissen B, Agace WW and Mowat AM: Resident and pro-inflammatory macrophages in the colon represent alternative context-dependent fates of the same Ly6Chi monocyte precursors. *Nat Immunol* 15: 929-937, 2014.
35. Zelenay S, van der Veen AG, Böttcher JP, Snelgrove KJ, Rogers N, Acton SE, Chakravarty P, Girotti MR, Marais R, Quezada SA, *et al*: Cyclooxygenase-dependent tumor growth through evasion of immunity. *Cell* 162: 1257-1270, 2015.
36. Grainger JR, Askenase MH, Guimont-Desrochers F, da Fonseca DM and Belkaid Y: Contextual functions of antigen-presenting cells in the gastrointestinal tract. *Immunol Rev* 259: 75-87, 2014.
37. de Jong JP, Voerman JS, van der Sluijs-Gelling AJ, Willemsen R and Ploemacher RE: A monoclonal antibody (ER-HR3) against murine macrophages. I. Ontogeny, distribution and enzyme histochemical characterization of ER-HR3-positive cells. *Cell Tissue Res* 275: 567-576, 1994.
38. de Jong JP, Leenen PJ, Voerman JS, van der Sluijs-Gelling AJ and Ploemacher RE: A monoclonal antibody (ER-HR3) against murine macrophages. II. Biochemical and functional aspects of the ER-HR3 antigen. *Cell Tissue Res* 275: 577-585, 1994.



This work is licensed under a Creative Commons Attribution-NonCommercial-NoDerivatives 4.0 International (CC BY-NC-ND 4.0) License.